Solar Energy Materials and Solar Cells xxx (xxxx) xxx–xxx

Contents lists available at ScienceDirect

Solar Energy Materials and Solar Cells

journal homepage: www.elsevier.com/locate/solmat

Electrochromic devices based on tungsten oxide films with honeycomb-like nanostructures and nanoribbons array

Dongyun Ma, Tailiang Li, Zhongping Xu, Lixiang Wang, Jinmin Wang*

School of Environmental and Materials Engineering, College of Engineering, Shanghai Polytechnic University, Shanghai 201209, China

ARTICLE INFO

Keywords:
Tungsten trioxide
Nanoribbons
Honeycomb nanostructures
Electrochromic

ABSTRACT

$(NH_4)_{0.33}WO_3$ nanoribbon films with different morphologies were directly grown on fluorine-doped tin oxide (FTO) glasses by using a simple hydrothermal method without a seed layer. By varying the reaction time, disordered nanoribbons array and ordered honeycomb-like structures woven from nanoribbons can be selectively synthesized. After annealing at 400 °C for 1 h, both of the two kinds of films are changed from $(NH_4)_{0.33}WO_3$ to WO_3, while the morphologies are well preserved. In comparison with the device based on disordered nanoribbons array film, a larger optical modulation (51.6% *vs.* 39.2% at 700 nm), faster switching speeds (t_c/t_b, 5.7/4.2 s *vs.* 9.6/6.5 s) and a higher coloration efficiency (60.9 $cm^2\,C^{-1}$ *vs.* 28.2 $cm^2\,C^{-1}$) are achieved for the device based on honeycomb-like structures film. It should be attributed to the large specific surface area and ordered porous structure of the ordered honeycomb-like nanostructures, which may bring a high diffusion rate and short diffusion path for the intercalation and deintercalation of Li^+ ions.

1. Introduction

Tungsten trioxide (WO_3), as a typical transition metal oxide, receives extensive attention because of its great potential applications in chromogenic [1,2], gas sensor [3,4], photocatalysis [5] and batteries [6]. Electrochromism is the phenomenon that a material can change its optical properties reversible by application of an electric field [7,8]. WO_3 has been extensively studied as an electrochromic (EC) material due to its excellent coloration effects and is widely used in smart windows, displays and anti-dazzling rear-view mirror [9,10].

The operation of WO_3-based EC devices refers to the reversible intercalation and deintercalation of electrons and ions, and this process is believed to have a great relation to the surface morphology and microstructure of WO_3 films. Thus nanostructured EC films with large specific surface area and porosity are required to achieve fast insertion/extraction kinetics and large ion storage capacity [11,12]. A variety of techniques have been successfully developed to fabricate nanostructured WO_3 films, including sol-gel method [13,14], electrodeposition [15,16], hydrothermal method [17,18], anodic oxidation [19] and magnetron sputtering [20]. Among them, hydrothermal approach has been used to synthesize various WO_3 nanostructures directly on a conductive substrate, such as nanowires [21–23], nanosheets [24,25], nanoribbons [26], nanorods [27,28] and three-dimensional (3D) nanostructures [29–32]. For example, one-dimensional WO_3 nanowire arrays have been prepared by Zhang et al. [33] using a template-free hydrothermal method and the enhanced EC performances were reported. Wang et al. [34] demonstrated that nanoflower-like 3D WO_3 structures can be prepared using the microwave-assisted hydrothermal process, and the photoelectrochemical performances were also investigated. However, a seed layer was necessary for growing the above-mentioned WO_3 nanostructures directly on conductive substrates. This crystal-seed-assisted hydrothermal process typically needs a fairly complicated process for preparing the seed layer. Moreover, the seed layer will lengthen the electron transport path leading to a slow response speed. Additionally, to our knowledge, there was no report on growing WO_3 nanoribbons array by a seed-layer-free hydrothermal process.

Herein, we report a simple hydrothermal approach to synthesize $(NH_4)_{0.33}WO_3$ nanoribbon films with different morphologies directly on fluorine-doped tin oxide (FTO) glasses without a seed layer. The growth mechanism of the as-prepared nanoribbon film from disordered array to ordered flower-like array is discussed. After annealing at 400 °C for 1 h, both of the two kinds of films are changed from $(NH_4)_{0.33}WO_3$ to WO_3, while the morphologies are well preserved. Compared with the device based on disordered nanoribbons array film, highly enhanced EC properties are obtained for the device based on honeycomb-like nanostructured film.

* Corresponding author.
E-mail address: wangjinmin@sspu.edu.cn (J. Wang).

http://dx.doi.org/10.1016/j.solmat.2017.06.009
Received 20 December 2016; Received in revised form 3 June 2017; Accepted 6 June 2017

2. Experimental

2.1. Materials

All chemicals involved in the study were of analytical grade without further purification, purchased from Sinopharm Chemical Reagent Co. Ltd (China). The FTO glass used in this work (Square resistance ≤8 Ω, Transmittance ≥82% in wavelength range of 400–800 nm) was cleaned by sequential sonication in acetone, ethanol and de-ionized water for 10 min, respectively.

2.2. Film preparation

The film was obtained by a typical hydrothermal process. The precursor solution for hydrothermal use was prepared by dissolving 0.3042 g of ammonium paratungstate hydrate ($H_{40}N_{10}O_{41}W_{12}{\cdot}xH_2O$, molecular weight 3042) and 6.3 g of oxalic acid dehydrate ($C_2H_2O_4{\cdot}2H_2O$) in 20 g of ethanol. The resulting mixture was sonicated for 15 min before transferred into a 50 mL Teflon-lined stainless-steel autoclave. A piece of FTO glass was placed into the autoclave and leaned on the wall with the conductive side facing down. Then the autoclave was sealed and maintained at 200 °C for 4–8 h. After synthesis, the as-synthesized film was cleaned with ethanol and dried in air; a honeycomb $(NH_4)_{0.33}WO_3$ nanoribbon array film was obtained. Finally, the WO_3 film can be achieved by annealing the as-synthesized $(NH_4)_{0.33}WO_3$ film in air at 400 °C for 1 h.

2.3. Device fabrication

The as-prepared WO_3 films were assembled into EC devices with same configuration of FTO glass/WO_3 film/1.0 mol L^{-1} $LiClO_4$ in propylene carbonate (PC)/FTO glass, and a 0.2 mm-thickness of double sided adhesive tape was used to seal the device.

2.4. Characterization

The phase identification of the products were investigated using X-ray diffraction (XRD, Cu Kα radiation, λ = 0.15418 nm). The morphology and structure of the as-synthesized products were characterized using field emission scanning electron microscopy (FESEM, Hitachi, S-4800, 10 kV, 10 μA), transmission electron microscopy (TEM, JEM 2100F, 200 kV), high-resolution TEM (HRTEM) and selected-area electron diffraction (SAED) patterns. Electrochemical measurements of the as-prepared WO_3 films were measured by an electrochemical workstation (Metrohm Autolab, AUT86311) with a three-electrode system (a WO_3 film, Pt sheet and Saturation calomel electrode (SCE) were used as the working electrode, counter electrode and reference electrode, respectively; 1.0 mol L^{-1} $LiClO_4$ in PC was used as the electrolyte). Cyclic voltammograms (CVs) were measured from −0.8 to 1.2 V with a scanning rate of 0.1 V s^{-1}. The coloration and bleaching of the assembled devices were tested by applying a potential of −0.8 V and 1.0 V for 15 s, respectively. The *in situ* transmittance spectrum of the WO_3 based devices were recorded by an UV–Vis spectrophotometer (PC SHIMADZU, UV-2600, Japan) over visible wavelength range from 400 to 800 nm, and the switching response curve was extracted at 700 nm.

3. Results and discussion

3.1. Structure and morphology

Thin films of $(NH_4)_{0.33}WO_3$ nanoribbons with different morphologies were directly grown on a FTO substrate using a simple hydrothermal method without a seed layer. Fig. 1 shows the XRD patterns of bare FTO glass (Fig. 1a) and the as-prepared films before and after annealing. It is confirmed from Fig. 1b that the films hydrothermally grown on FTO glasses are $(NH_4)_{0.33}WO_3$ before annealing. All of the peaks (excluding the peaks of bare FTO glass) can be indexed to hexagonal phase of $(NH_4)_{0.33}WO_3$ (JCPDS no. 42-0452), which indicates that pure $(NH_4)_{0.33}WO_3$ is obtained. After annealing at 400 °C for 1 h, $(NH_4)_{0.33}WO_3$ is completely changed to WO_3 (Fig. 1c), with all the peaks (excepting the peaks of bare FTO glass) corresponding to the hexagonal phase of WO_3 (JCPDS no. 85-2460). The sharp peaks also indicate that the as-synthesized films were well crystallized.

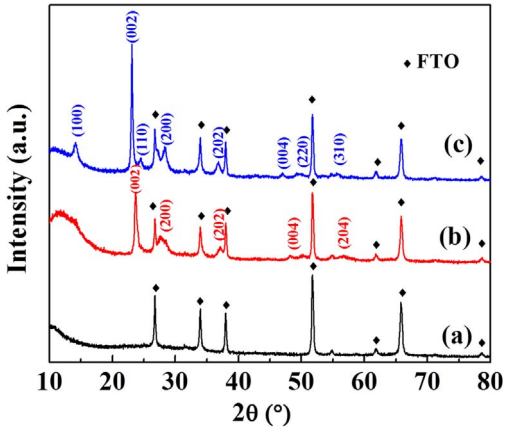

Fig. 1. XRD patterns of (a) bare FTO glass, (b) film hydrothermally grown on FTO glass and (c) after subsequently annealing at 400 °C for 1 h.

The morphology and microstructure of the hydrothermally grown $(NH_4)_{0.33}WO_3$ films were characterized by FESEM and TEM. Fig. 2 shows FESEM images of the films obtained at different hydrothermal reaction times. It can be seen from Fig. 2a that the film is composed of nanoribbon arrays after hydrothermal growth at 200 °C for 4 h. The nanoribbons are 150–300 nm in width and ~25 nm in thickness (Fig. 2a). The nanoribbon arrays are disordered and looked like bushy grass. When the reaction time is increased to 6 h, there is no significant change in width and thickness for nanoribbons. Interestingly, the nanoribbons began to interweave with each other to form a honeycomb-like structure (Fig. 2b). The perfect honeycomb-like nanostructure was eventually formed when the reaction time was prolonged to 8 h and uniform large-area $(NH_4)_{0.33}WO_3$ film with ordered porous nanostructure was obtained (Fig. 2c and d). The diameter of pores is about 2–4 μm and the three-dimensional (3D) braid structure woven from nanoribbons can be clearly seen from Fig. 2e. Moreover, a tripod structure is formed at the junction of three adjacent pores (Fig. 2f), which plays an important role in guaranteeing the structural stability of whole morphology. As shown in cross-sectional view, the thickness of the FTO layer is about 0.8 μm, and the thickness of the as-prepared film is about 4.0 μm (Fig. 2h).

The hydrothermally grown $(NH_4)_{0.33}WO_3$ nanoribbons were further studied by TEM analysis, as shown in Fig. 3. The representative TEM image (Fig. 3a) confirms that the as-prepared films are made of $(NH_4)_{0.33}WO_3$ nanoribbons, and the width and thickness of the nanoribbons are 150–300 nm and ~25 nm, respectively, which is in good agreement with the FESEM results. The HRTEM image (Fig. 3b) reveals clear lattice fringes with an interplanar distance of about 0.375 nm, which corresponds to the *d*-spacing of the (002) planes of hexagonal $(NH_4)_{0.33}WO_3$, indicating the high crystallinity and preferential growth direction of the nanoribbons.

The composition of the precursor solution also plays an important role in controlling the morphology and size of the hydrothermal products. It is known that $H_{40}N_{10}O_{41}W_{12}{\cdot}xH_2O$ is sparingly soluble in ethanol. With increasing the hydrothermal reaction temperature, the water molecules lost from oxalic acid dehydrate promoted the hydrolysis of $H_{40}N_{10}O_{41}W_{12}{\cdot}xH_2O$. Additionally, the oxalic acid acts as a capping agent for growing $(NH_4)_{0.33}WO_3$ nanoribbons. There have been some reports of using oxalic acid as the capping agent for growing one-